Molecular Biology of the Cell
Vol. 21, 3475–3486, October 1, 2010

The Rapamycin-sensitive Phosphoproteome Reveals That TOR Controls Protein Kinase A Toward Some But Not All Substrates

Alexandre Soulard,* Alessio Cremonesi,* Suzette Moes, Frédéric Schütz, Paul Jenö, and Michael N. Hall

Biozentrum, University of Basel, CH-4056 Basel, Switzerland

Submitted March 3, 2010; Revised July 6, 2010; Accepted August 4, 2010
Monitoring Editor: Daniel Lew

Regulation of cell growth requires extensive coordination of several processes including transcription, ribosome biogenesis, translation, nutrient metabolism, and autophagy. In yeast, the protein kinases Target of Rapamycin (TOR) and protein kinase A (PKA) regulate these processes and are thereby the main activators of cell growth in response to nutrients. How TOR, PKA, and their corresponding signaling pathways are coordinated to control the same cellular processes is not understood. Quantitative analysis of the rapamycin-sensitive phosphoproteome combined with targeted analysis of PKA substrates suggests that TOR complex 1 (TORC1) activates PKA but only toward a subset of substrates. Furthermore, we show that TORC1 signaling impinges on BCY1, the negative regulatory subunit of PKA. Inhibition of TORC1 with rapamycin leads to BCY1 phosphorylation on several sites including T129. Phosphorylation of BCY1 T129 results in BCY1 activation and inhibition of PKA. TORC1 inhibits BCY1 T129 phosphorylation by phosphorylating and activating the S6K homolog SCH9 that in turn inhibits the MAP kinase MPK1. MPK1 phosphorylates BCY1 T129 directly. Thus, TORC1 activates PKA toward some substrates by preventing MPK1-mediated activation of BCY1.

INTRODUCTION

Cells regulate their growth in response to nutrients. To achieve this growth control, cells sense and transduce nutrient signals to coordinate several processes including transcription, ribosome biogenesis, translation, nutrient transport and metabolism, and cell morphogenesis and autophagy. In *Saccharomyces cerevisiae*, the TOR (Target of Rapamycin) and cAMP-dependent protein kinase A (PKA) signaling pathways are the two major pathways that transduce nutrient signals to regulate cell growth (De Virgilio and Loewith, 2006; Santangelo, 2006; Soulard *et al.*, 2009).

TOR is found in two highly conserved and functionally distinct complexes corresponding to two effector signaling branches (Wullschleger *et al.*, 2006). Rapamycin-sensitive TOR Complex 1 (TORC1) mediates temporal control of cell growth in response to nutrients by promoting anabolic processes such as translation and ribosomal protein (RP) gene expression and by antagonizing catabolic processes such as autophagy, ubiquitin-dependent protein degradation, and mRNA degradation (Crespo and Hall, 2002; Loewith *et al.*, 2002; Reinke *et al.*, 2004; De Virgilio and Loewith, 2006). In addition, TORC1 regulates lifespan (Kaeberlein *et al.*, 2005). Rapamycin-insensitive TOR Complex 2 (TORC2) mediates spatial control of cell growth by regulating actin cytoskeleton dynamics, ceramide metabolism, and cell wall integrity (De Virgilio and Loewith, 2006; Aronova *et al.*, 2008; Cybulski and Hall, 2009).

PKA in yeast is part of the RAS-cAMP signaling cascade that controls various growth-related processes in response to glucose (Santangelo, 2006). Like TORC1, the PKA pathway regulates translation, ribosome biogenesis, autophagy, stress responses, glucose metabolism, and lifespan (Santangelo, 2006). The PKA catalytic subunit is encoded by the three homologous and partly redundant genes *TPK1*, *TPK2*, and *TPK3*. The PKA regulatory subunit that controls PKA in response to cAMP is encoded by *BCY1* (Cannon and Tatchell, 1987; Toda *et al.*, 1987a,b). In the absence of glucose (i.e., a fermentable carbon source), two BCY1s bind two TPKs to form a catalytically inactive heterotetrameric complex. In the presence of glucose, adenylate cyclase is activated and produces cAMP from ATP. cAMP in turn activates PKA by binding BCY1 and releasing it from TPK (Johnson *et al.*, 1987; Santangelo, 2006). Furthermore, both TPK1 and BCY1 shuttle between the cytoplasm and the nucleus in growing cells, with BCY1 mainly in the nucleus and TPK1 primarily in the cytoplasm (Griffioen *et al.*, 2000, 2001; Schmelzle *et al.*, 2004).

TORC1 and PKA regulate common target proteins to activate or inhibit the same biological processes. For example, both TORC1 and PKA regulate the nuclear localization of SFP1 and CRF1, two transcription cofactors involved in RP gene expression (Jorgensen *et al.*, 2004; Marion *et al.*, 2004; Martin *et al.*, 2004; Schawalder *et al.*, 2004; Wade *et al.*, 2004). Similarly, the stress-inducible transcription factors MSN2

This article was published online ahead of print in *MBoC in Press* (http://www.molbiolcell.org/cgi/doi/10.1091/mbc.E10–03–0182) on August 4, 2010.

* These authors contributed equally to this work.

Address correspondence to: Michael N. Hall (m.hall@unibas.ch).

Supplemental Material can be found at:
http://www.molbiolcell.org/content/suppl/2010/08/10/E10-03-0182.DC1

and MSN4 are dephosphorylated and rapidly accumulate in the nucleus upon TORC1 or PKA inhibition (Gorner *et al.*, 1998; Beck and Hall, 1999). Inhibition of either TORC1 or PKA also leads to the dephosphorylation, nuclear accumulation, and activation of MAF1, a repressor of RNA polymerase III (Moir *et al.*, 2006; Huber *et al.*, 2009; Lee *et al.*, 2009). Seemingly conflicting models have been proposed to account for the overlapping regulation by TORC1 and PKA. According to one model, TORC1 and PKA are in distinct but parallel pathways that converge on common target proteins or processes. For example, TORC1 and PKA independently regulate MSN2 and ATG13 phosphorylation (Santhanam *et al.*, 2004; Stephan *et al.*, 2009). Alternatively, several findings suggest that TORC1 is an activator of PKA, placing the two kinases in the same signaling pathway. First, hyperactivation of the RAS-cAMP-PKA pathway suppresses a TORC1 deficiency, whereas down-regulation of the PKA pathway leads to increased rapamycin sensitivity (Schmelzle *et al.*, 2004; Zurita-Martinez and Cardenas, 2005). Second, TORC1 controls RP gene expression via PKA (Martin *et al.*, 2004; Schmelzle *et al.*, 2004). Third, the AGC kinase SCH9, which is a direct substrate of TORC1, was initially identified as a multicopy suppressor of mutations that reduce PKA activity (Toda *et al.*, 1988; Urban *et al.*, 2007). Fourth, inactivation of TORC1 by rapamycin causes a rapid accumulation of the PKA catalytic subunit TPK1 in the nucleus (Schmelzle *et al.*, 2004). All together, the above findings are inconsistent with a single model to explain the common regulation by TORC1 and PKA.

The cell wall integrity pathway consists of the RHO1-PKC1-BCK1-MKK1/2-MPK1 signaling cascade. This pathway allows yeast cells to adapt their growth and shape in response to cell wall stress (Levin, 2005). Recently, several reports have linked the cell wall integrity pathway to both TORC1 and PKA signaling. For example, inactivation of TORC1 leads to the phosphorylation and activation of the mitogen-activated protein (MAP) kinase MPK1, and several components of the cell wall integrity pathway show genetic interactions with components of the PKA pathway (Verna *et al.*, 1997; Krause and Gray, 2002; Torres *et al.*, 2002; Park *et al.*, 2005; Kuranda *et al.*, 2006). However, a molecular link between TORC1 and PKA via the cell wall integrity pathway is unknown.

To better understand the relationship between TORC1 and PKA, we further investigated the effect of TORC1 inhibition on PKA. We observed, by large-scale quantitative phosphoproteome analysis and targeted experiments, that a distinct subset of PKA target sites become dephosphorylated upon rapamycin treatment. To investigate the mechanism by which TORC1 controls PKA, we focused on the PKA regulatory subunit BCY1. TORC1 regulates PKA by inhibiting phosphorylation of many sites in BCY1 between a dimerization domain and the cAMP-binding domain. TORC1 inhibits BCY1 phosphorylation via SCH9 and the MAP kinase MPK1. Thus, we define a signaling cascade in which TORC1 is upstream of PKA toward at least some substrates.

MATERIALS AND METHODS

Strains, Plasmids, Media, and Genetic Manipulations

The *S. cerevisiae* strains and plasmids used in this study are listed in Supplementary Tables 1 and 2, respectively. All strains from our laboratory are isogenic with TB50. Yeast manipulations, including cell cultures, sporulation, tetrad dissections, and genetic techniques, were carried out essentially as described by Guthrie and Fink (1991). The media were YPD (1% yeast extract, 1% peptone, 2% dextrose, plus 2% agar for solid media) and minimal synthetic medium (SD; yeast nitrogen base at 6.7 g/l, 2% dextrose, relevant amino acids and 2% agar for plates). YP medium was used for the glucose depletion experiment. SDS in YPD was 0.01%. Cells were treated with rapamycin at 200 ng/ml final concentration (added from a 1 mg/ml stock solution in 90% ethanol–10% Tween20) and/or 8-Bromo-cAMP at 5 mM final concentration (from 250 mM stock solution in water). Before 8-Bromo-cAMP treatment, cells were centrifuged and resuspended in 5 ml of the required medium. In most experiments, yeast strains carrying a plasmid were precultured in SD medium lacking the corresponding amino acids for plasmid maintenance and subsequently diluted into YPD medium. Cells were then grown for 4–5 h (to OD_{600} about 0.8) before treatment. For SILAC labeling, yeast cells were grown in SD medium containing $^{13}C_6$-arginine and $^{13}C_6$,$^{15}N_2$-L-lysine (Cambridge Isotope Laboratories, Andover, MA). Transformations of *S. cerevisiae* cells were according to the lithium acetate method with single-strand carrier DNA and dimethyl sulfoxide (DMSO; Hill *et al.*, 1991). All deletion and genomically tagged strains were constructed by PCR-based gene targeting (Wach *et al.*, 1994). One-step site directed mutagenesis was performed as described previously (Zheng *et al.*, 2004).

Fluorescence Microscopy

Fluorescence microscopy and indirect immunofluorescence on whole fixed cells was performed as described previously (Schmelzle *et al.*, 2004).

Protein Extraction, Immunoprecipitation, Western Blotting, and Phosphatase Treatment

Protein extracts were prepared from exponentially growing cells. At least 25 OD cells were broken in a bead beater in lysis buffer (PBS containing 0.5% Tween 20 and 10% glycerol) containing 1× Roche protease inhibitor cocktail, 1 mM PMSF, and phosphatase inhibitors (10 mM NaF, 10 mM NaN_3, 10 mM *p*-nitrophenyl phosphate, 10 mM sodium pyrophosphate, and 10 mM β-glycerophosphate). hemagglutinin (HA)-, MYC-, or tandem affinity purification (TAP)-tagged proteins were immunoprecipitated from cell extracts with protein A-Sepharose beads coupled to anti-HA antibody (12C2A), protein G-Sepharose beads coupled to anti-MYC antibody (1-9E10.2), or human IgG-Sepharose beads (GE Healthcare, Waukesha, WI), respectively. For the phosphatase experiment, beads were further washed with phosphatase buffer (50 mM Tris-Cl, pH 7.5, 1 mM $MgCl_2$), resuspended in 100 μl phosphatase buffer, and incubated for 10 min at 30°C. Twenty units of calf intestine alkaline phosphatase was added, and the reaction was incubated for 15 min 30°C. For the gel-shift assay, the acrylamide-bisacrylamide ratio for SDS-PAGE was changed to 172:1. The primary antibodies for Western blotting were as follows: anti-HA (mouse monoclonal, 12C2A), anti-MYC (mouse monoclonal, 1-9E10.2), anti-protein A (rabbit polyclonal, Sigma-Aldrich, St. Louis, MO), anti-BCY1 (goat polyclonal, Bcy1 [yN19] sc-6765, Santa Cruz Biotechnology, Santa Cruz, CA), anti-RxxS/T (rabbit polyclonal phospho-[Ser/Thr] PKA substrate antibody no. 9621, Cell Signaling, Beverly, MA), anti-RRxS/T (phospho-PKA Substrate [RRXS/T; 100G7E], rabbit mAb no. 9624, Cell Signaling), anti-MPK1 (goat polyclonal, Mpk1 [yC-20] sc-6803, Santa Cruz Biotechnology), anti-phospho MPK1 (rabbit polyclonal, phospho-p44/42 MAPK [Thr202/Tyr204] antibody no. 9101, Cell Signaling). (The phosphorylated residues are underlined.)

Identification of Phosphorylation Sites in BCY1

Wild-type TB50a cells or cells expressing N-terminally H- tagged BCY1 (SA094) were grown in 500 ml YPD to $OD_{600\ nm}$ of 1 and treated with rapamycin (200 ng/ml) or drug vehicle for 90 min. Cells were broken with glass beads with RIPA buffer (25 mM Tris-Cl, pH 7.5, 150 mM NaCl, 1% Nonidet NP-40, 1% Na-deoxycholate) supplemented with 1× Roche protease inhibitor cocktail and phosphatase inhibitors (10 mM NaF, 0.2 μM okadaic acid, and 20 nM calyculin A). HA-tagged BCY1 was immunoprecipitated from 40 mg of total protein extract with 1 μl of monoclonal anti-HA antibody (HA.11; Covance, Princeton, NJ) at 4°C for 18 h followed by incubation with 100 μl of Dynabeads protein G (Invitrogen, Carlsbad, CA) for 4 h at 4°C. The beads were washed and HA-BCY1 was eluted from the beads with 10 μl 3 M urea, and 20 mM DTT for 10 min at room temperature. HA-BCY1 was digested with trypsin for 18 h at 37°C. Proteolysis was stopped with 8.4 μl acetic acid, and the peptides were dried in a Speed Vac. Phosphopeptides were enriched with TiO_2-magnetic beads (Perkin Elmer-Cetus, Waltham, MA) according to the manufacturer's instructions. The final peptides were analyzed by capillary liquid chromatography tandem MS (LC/MS/MS) using a 300SB C-18 column (0.3 × 50 mm; Agilent Technologies, Basel, Switzerland) connected on line to an LTQ-Orbitrap hybrid instrument (Thermo Finnigan, San Jose, CA; see below).

Glycogen Staining

Staining of intracellular glycogen was performed with iodine vapor as previously described (Barbet *et al.*, 1996).

MPK1 Kinase Assay

Yeast cells expressing HA-tagged MPK1 were grown in 500 ml YPD to an $OD_{600\ nm}$ of 1 and then treated for 30 min with rapamycin or drug vehicle. Protein extraction, immunoprecipitation, and in vitro kinase assays were

done as previously describe with slight modifications (Watanabe *et al.*, 1997). Modified RIPA buffer (25 mM Tris-Cl, pH 7.5, 150 mM NaCl, 1% Nonidet NP-40, 1% Na-deoxycholate) was used to break the cells, and 20 mg of total protein extract was used for the immunoprecipitation. The TB50a wild-type strain was used as mock control. A fraction of total lysate (20 μg) was kept to check MPK1-HA expression and phosphorylation on Western blots.

Zymolyase Sensitivity Assay

Zymolyase sensitivity was tested as reported (Ho *et al.*, 2005).

Phosphoproteome Analysis: SILAC Labeling and Protein Extraction

Two 200-ml cultures of YPJ2 cells (derived from TB50a) were grown at 30°C in SD medium supplemented with either 30 mg/l $^{12}C_6$-arginine and $^{12}C_6$-lysine ("light" culture) or $^{13}C_6$ L-arginine and $^{13}C_6$,$^{15}N_2$ L-lysine ("heavy" culture) to an optical density (600 nm) of ~0.7. The heavy culture was treated for 15 min with 200 nM rapamycin, whereas the light culture was treated mock-treated with the vehicle for 15 min. To produce reliable quantitative data, four biological replicates were performed, always starting from a single yeast clone. In one of the four experiments the labeling was swapped to check that the labeling influences neither protein expression nor phosphorylation. After rapamycin treatment, both cell cultures were centrifuged at 3500 × *g* for 10 min at 4°C, and the cell pellets were washed with ice-cold water.

The cell pellets were individually resuspended in 2 ml ice-cold lysis buffer, containing 100 mM Tris-HCl, pH 7.5, 2.5% SDS, 10% glycerol, 1× protease inhibitor cocktail (Roche Diagnostics, Indianapolis, IN; dissolved in ddH_2O), 1× phosphatase inhibitor cocktail 1 (Sigma-Aldrich, dissolved in 100% DMSO) and 1 mM PMSF (AppliChem, Darmstadt, Germany; dissolved in 100% DMSO). Total protein extraction from either light or heavy cultures was performed by bead-beating as described above. The lysates were cleared at 15,000 × *g* for 10 min at 4°C. Protein concentrations in the extracts were measured with the bicinchonic acid assay (BCA, Sigma-Aldrich). About 2.5 mg of light- or heavy-labeled protein extracts were mixed and after addition of 6× sample buffer were incubated at 95°C for 5 min and subjected to preparative electrophoresis.

Phosphoproteome Analysis: Protein Fractionation and In-Gel Digestion

The mixed protein extracts were separated on a preparative 10% SDS slab gel. After electrophoresis, the gel was stained with SimplyBlue SafeStain (Invitrogen). The gel was then sliced horizontally into 16 regions, and the individual slices were further diced into 1-mm^3 cubes. The gel pieces were destained overnight in 1 ml 50% acetonitrile/50 mM NH_4HCO_3, dehydrated with 500 μl 100% acetonitrile, and dried in a speed-vac. The proteins were in-gel reduced in 1 ml 50 mM NH_4HCO_3 containing 10 mM DTT at 55°C for 60 min. Alkylation was done in 1 ml 50 mM iodoacetamide (in 50 mM NH_4HCO_3) in the dark for 30 min. After the gel pieces were washed three times with 1 ml 50% acetonitrile/50 mM NH_4HCO_3, they were dehydrated with 500 μl 100% acetonitrile, dried in a speed-vac, and then rehydrated on ice for 1 h in 1 ml 50 mM NH_4HCO_3, pH 8.0, containing 15 ng/μl trypsin (Sigma). Digestion was carried out overnight at 37°C. Supernatants were collected in fresh tubes and the gel pieces were extracted three times with 50% acetonitrile/5% formic acid, followed by a final extraction with 100% acetonitrile. The volume of the individual digests was reduced in a speed-vac to ~10 μl to which 290 μl 1% acetic acid was added. A small drop was spotted onto pH paper, and if necessary the pH was adjusted to 2.0–2.5 with 10% acetic acid.

Phosphoproteome Analysis: Peptide Desalting and Phosphopeptide Enrichment

For phosphopeptide enrichment, the digests were desalted on C18 MacroSpin columns (500 μl packed resin, The Nest Group, Southborough, MA) according to the manufacturer's instructions. The peptides were eluted from the cartridge with 600 μl 60% acetonitrile/1% acetic acid. The eluates were speed-vac dried to ~10 μl to which 90 μl IMAC-buffer (30% acetonitrile/250 mM acetic acid) was added. One microliter of each digest was diluted 200-fold with 2% acetonitrile/0.1% acetic acid, and 10 μl was analyzed by LC/MS/MS for expression analysis.

For phosphopeptide enrichment, 40 μl IMAC slurry (PHOS-Select, Sigma-Aldrich) was washed five times with 1 ml IMAC-buffer and then loaded into a constricted GELoader tip (Thingholm *et al.*, 2006). The desalted digests were applied to the IMAC columns. The flow-throughs were collected and reloaded five times to ensure maximal binding. The resin was washed three times with 150 μL IMAC-buffer. Bound phosphopeptides were eluted with three successive 70-μl desorptions of 50 mM KH_2PO_4, pH 10.0, into Eppendorf tubes containing 30 μl 10% formic acid. The IMAC eluates were desalted on disposable C18 MicroSpin columns (MA100 μl packed volume, The Nest Group) according to the manufacturer's instructions. After elution with 200 μl 60% acetonitrile/1% acetic acid, the volume was reduced in a speed-vac to ~10 μl, and the phosphopeptides were diluted with 40 μl 2% acetonitrile/0.1% formic acid for LC-MS/MS analysis.

Phosphoproteome Analysis: LC-MS/MS Analysis

LC-MS/MS analysis was performed on an LTQ-Orbitrap hybrid instrument (Thermo Scientific). Ten microliters of IMAC eluate was injected with an autosampler (CTC Analytics, Agilent Technologies, Basel, Switzerland) onto a C18 trapping column (300SB C-18 0.3 × 50 mm, Agilent Technologies) that was connected to a separation column (0.1 mm × 10 cm) packed with Magic 300 Å C18 reverse-phase material (5-μm particle size, Michrom Bioresources, Auburn, CA). A linear 80-min gradient from 2 to 50% solvent B (80% acetonitrile/0.1% acetic acid) in solvent A (2% acetonitrile/0.1% acetic acid) was delivered with a Rheos 2200 pump (Flux Instruments, Basel, Switzerland) at a flow rate of 100 μl/min. A precolumn split was used to reduce the flow to ~300 nl/min. The eluting peptides were ionized at 1.7 kV.

The LTQ-Orbitrap was operated in data-dependent mode. A survey scan between m/z 375 and 1600 was acquired in profile mode in the Orbitrap at 60,000 resolution, and the 10 most abundant ions were then selected for fragmentation in the LTQ part of the instrument at normalized collision energy of 35%. To facilitate fragmentation of phosphopeptides, a CID scan was followed by multistage activation. Singly charged ions were omitted from fragmentation, and previously selected ions were dynamically excluded for 25 s. Scan-to-scan calibration was allowed by setting the lock mass to m/z 445.120025 (Olsen *et al.*, 2005).

Phosphoproteome Analysis: Database Search, Statistics, and Quantitation

To obtain statistically relevant quantitative phosphoproteomes, four independent SILAC experiments from either untreated or rapamycin-treated cell cultures were collected. The MS data were processed with MaxQuant (version 1.0.12.31;Max Plank Institute of Biochemistry, Martinsreid, Germany) and searched with the Mascot search engine (version 2.2.04, Matrix Science, London, United Kingdom) against a databank containing 31,426 protein sequences (Perkins *et al.*, 1999; Cox and Mann, 2008; Cox *et al.*, 2009). The databank contained forward and reverse *S. cerevisiae* sequences as well as common contaminants (Swiss-Prot; from European Bioinformatics Institute; http://www.ebi.ac.uk/uniprot). Precursor ion and fragment ion mass tolerances were set to 7 ppm and 0.6 Da, respectively. Two missed cleavages were allowed. Dynamic modifications were oxidation for methionine and phosphorylation of serine, threonine, and tyrosine, whereas cysteine carbamidomethylation was set as fixed modification. To increase identification stringency only peptides with a Mascot score above 20 were accepted. In addition, only MS/MS spectra with a posterior error probability (PEP) below 0.1 were accepted (Hilger *et al.*, 2009). The MaxQuant output was simplified by replacing oxidized with unmodified methionines. In addition, proteins matching the same (phospho)peptides were merged into one hit. Gene products of the Ty retrotransposons and the *S. cerevisiae* virus L-A were manually removed. For expression analysis, all peptides belonging to the same protein were merged, whereas for phosphorylation analysis, all redundant phosphopeptides containing the same phosphorylation site(s) were grouped together. To evaluate the biological reproducibility of the four experiments, the ratios of the heavy labels to light labels obtained in one experiment were compared with all other experiments. A high correlation was obtained for all four experiments, indicating good reproducibility throughout the entire study (Supplementary Figure 1A). To find changes in expression or phosphorylation that are above the experimental error, an experiment was done without rapamycin treatment. The SILAC ratios were $\log_2$ transformed, and the experimental average and SDs were found to be 0.02 and 0.28 ($SD_{control}$), respectively. Then, the SILAC ratios of the four cell cultures were $\log_2$ transformed, and for those proteins or phosphopeptides that occurred in more than one experiment, a 95% confidence interval was calculated along with the median of the log ratios to assess the influence of outliers. Up-regulation of expression or phosphorylation was considered significant when the lower confidence limits were more than or equal to 0.56 (twice the $SD_{control}$). Likewise, down-regulation of protein expression or the extent of phosphorylation was considered significant when the upper confidence limit was less than or equal to −0.56. Those proteins or phosphopeptides that were found in only one experiment but also that showed a large change in abundance or phosphorylation were accepted only if the $\log_2$-transformed ratios were more than 1.12 or less than −1.12 (four times $SD_{control}$). The choice of these two thresholds (two and four times the SD of the control, respectively) was made in a conservative way, in order to minimize the number of false positive we obtained. Notably, by using these two selection criteria, among the regulated hits we found many proteins that were already known to be controlled by TORC1 (Supplementary Figure 1, C and D).

RESULTS

PKA Sites Are Primary Targets for TORC1-dependent Phosphorylation

Although it is known that TORC1 regulates many cellular processes, the molecular mechanisms by which TORC1 signals to these diverse processes are often not well under-

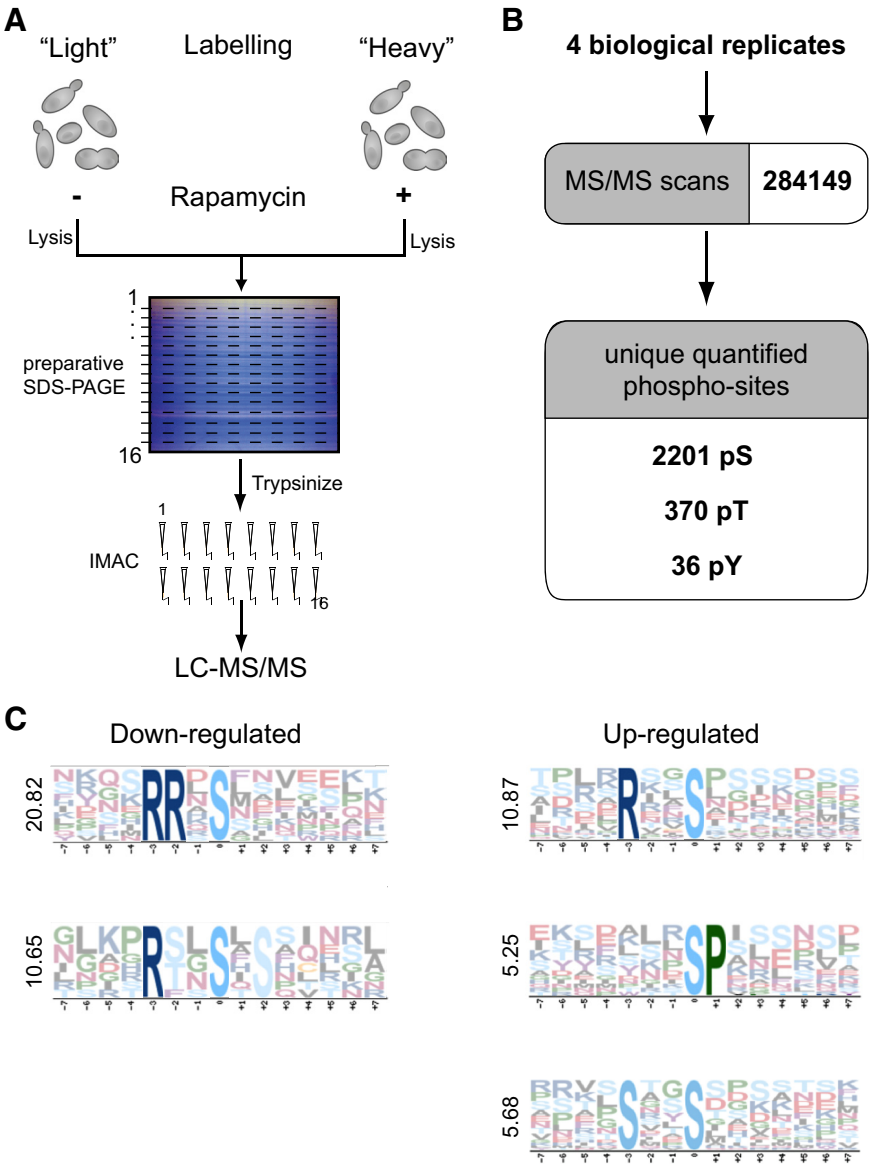

Figure 1. Quantitative analysis of the rapamycin-sensitive phosphoproteome by SILAC. (A) Schematic overview of the experimental approach for the identification of TORC1 regulated phosphorylation sites in *S. cerevisiae*. Two yeast cultures (strain YPJ2) were metabolically labeled with $^{12}C_6$-$^{14}N_2$-lysine/$^{12}C_6$-arginine (light) or $^{13}C_6$-$^{15}N_2$-lysine/$^{13}C_6$-arginine (heavy). The heavy culture was treated for 15 min with rapamycin. Extracts were mixed in a 1:1 ratio and separated by preparative SDS-PAGE. The gel was horizontally sliced into 16 sections and in-gel–digested, and phosphopeptides were IMAC-enriched and analyzed in an LTQ-Orbitrap. (B) Merged data from the four experiments revealed 972 phosphoproteins, corresponding to 2487 unique phosphopeptides and 2607 unique phosphosites. (C) Analysis by Motif-X of all regulated phosphopeptides.

stood. In particular, very few substrates of either TORC1 or its direct effectors such as the AGC kinase SCH9 are known. To identify proteins whose phosphorylation changes in a TORC1-dependent manner, we performed unbiased quantitative phosphoproteomic analysis by stable isotope labeling with amino acids in cell culture (SILAC; Ong *et al.*, 2002). Extracts from rapamycin-treated untreated yeast cells were separated by preparative SDS gel electrophoresis, phosphopeptides were enriched by IMAC, and the resulting phosphopeptide pools were analyzed by LC-MS/MS (Figure 1A). Unique phosphopeptides (n = 2487) and unique phosphorylation sites (n = 2607), corresponding to 972 phosphoproteins, were identified and quantified (Figure 1B and Supplementary Table 3). Our phosphoproteome compares favorably to previously published yeast phosphoproteomes (Gruhler *et al.*, 2005; Li *et al.*, 2007; Wilson-Grady *et al.*, 2008) and includes both high- and low-abundance phosphoproteins (Supplementary Figure 1B; Ghaemmaghami *et al.*, 2003). Of the 972 phosphoproteins identified (Supplementary Table 3), 78 were significantly hyperphosphorylated, and 55 were hypophosphorylated upon rapamycin treatment (Supplementary Tables 4 and 5, respectively). To accurately quantify the changes in phosphorylation, the fold change in phosphorylation was systematically compared with the fold change in expression for each protein (Supplementary Tables 6–8). Analysis of the data revealed that many rapamycin-regulated phosphoproteins had been already genetically or biochemically linked to TORC1 signaling (Supplementary Figure 1, C and D), providing further validation of our phosphoproteome. During the preparation of this manuscript, another study describing the rapamycin-regulated phosphoproteome in yeast was published (Huber *et al.*, 2009). A comparison of the two studies revealed surprisingly little overlap. Although the total number of rapamycin-regulated proteins was very similar in the two studies (133 vs. 129), only 29 proteins were common to both studies (Supplementary Figure 1, C and D). Thus, the two studies provide different but complementary rapamycin-regulated phosphoproteomes.

To determine if TORC1 controls phosphorylation of specific motifs, we analyzed the sequences surrounding the rapamycin-regulated phosphosites, with the Motif-X algorithm (Schwartz and Gygi, 2005). For the peptides

Table 1. Proteins for which phosphorylation decreased at PKA consensus motif RRxS after rapamycin treatment

Protein	Phospho site[a]	Description[b] (SGD)
FRA1	S 56 (0.48 ± 0.16)	Protein involved in negative regulation of transcription of iron regulon
GCN2	S 577 (0.18 ± 0.02)	eIF2 kinase regulating translation in response to starvation
KCS1	S 537 (0.42)	Inositol hexakisphosphate (IP6) and inositol heptakisphosphate (IP7) kinase
KSP1	S 827 (0.27 ± 0.01) S 883, S 884 (0.11) S 884 (0.40)	Ser/thr protein kinase required for haploid filamentous growth
LHP1	S 19 (0.51 ± 0.13)	RNA-binding protein required for maturation of tRNA and U6 snRNA precursors
MAF1	S 90 (0.25 ± 0.08) S 209 (0.29)	Negative regulator of RNA polymerase III in response to nutrients and stress
MKS1	S 518 (0.43 ± 0.18)	Negative transcriptional regulator involved in Ras-cAMP and lysine biosynthetic pathways, and nitrogen regulation
SSD1	S 164 (0.56 ± 0.07)	Maintenance of cellular integrity, interacts with components of the TOR pathway
VTC2	S 583 (0.24 ± 0.03)	Subunit of the vacuolar transporter chaperone (VTC) complex involved in membrane trafficking
YJL016W	S 350 (0.50 ± 0.02)	Putative protein of unknown function

[a] For each protein the coordinate of the regulated phospho-site and the fold-increase the average ratio (±SD) are given in parentheses. No SD indicates that the phospho-sites were identified in only one experiment.

[b] The description of the function of the protein is given according to the SGD with adaptation.

whose phosphorylation was down-regulated upon rapamycin treatment, the top scoring target motif was RRxS (the phosphorylated residue is underlined; Figure 1C). This motif was underrepresented in the phosphopeptides whose phosphorylation was up-regulated (Figure 1C). The related motif RxxS appeared in both the up- and down-regulated phosphopeptides (Figures 1C). Finally, the two motifs SP and SxxS were also represented, but only in the up-regulated peptides. Examination of the rapamycin-sensitive phosphoproteome presented by Huber *et al.* (2009) revealed a similar bias toward RRxS sites for down-regulated phosphopeptides (Supplementary Table 9). Thus, RRxS is a primary target motif for TORC1-dependent phosphorylation.

Importantly, RRxS/T is the consensus target motif specifically recognized and phosphorylated by PKA (Shabb, 2001; Budovskaya *et al.,* 2005). Of the 55 proteins whose phosphorylation was decreased upon rapamycin-treatment, 10 were hypophosphorylated at this PKA target motif. The 10 proteins were FRA1, GCN2, KCS1, KSP1, LHP1, MAF1, MKS1, SSD1, VTC2, and YJL016W (Table 1). FRA1, KSP1, LHP1, MAF1, and SSD1 have been shown to be PKA targets in vitro (Budovskaya *et al.,* 2005; Ptacek *et al.,* 2005). MAF1 is phosphorylated and negatively regulated by PKA and TORC1 in vivo (Moir *et al.,* 2006; Huber *et al.,* 2009; Lee *et al.,* 2009; Wei *et al.,* 2009). The localization of the protein kinase KSP1 is influenced by PKA (Bharucha *et al.,* 2008), and GCN2, KCS1, KSP1, LHP1, MKS1, and SSD1 have been linked to TORC1 and/or PKA signaling either genetically or biochemically (SGD project; *Saccharomyces* Genome Database; http://www.yeastgenome.org/; Xie *et al.,* 2005; Huber *et al.,* 2009). Thus, TORC1 appears to mediate phosphorylation of PKA target sites.

It is also important to note that many phosphorylated PKA target motifs in our phosphoproteome were not affected by rapamycin treatment (Supplementary Table 3). These included the PKA sites in the three well-known PKA targets MSN2, BCY1, and NTH1 (Supplementary Table 3). Thus, TORC1 appears to mediate phosphorylation of only a subset of PKA target sites.

TORC1 Activates PKA toward Certain Substrates

The above findings suggested that TORC1 activates PKA at least toward a subset of substrates. To investigate whether TORC1 indeed activates PKA, we performed targeted analyses of individual PKA substrates. In particular, we investigated the effect of rapamycin treatment on the in vivo steady-state phosphorylation of the known or suspected PKA substrates MAF1, YPK3, and KSP1. We probed the phosphorylation of these PKA substrates with an antibody that specifically recognizes a phosphorylated consensus PKA target motif (RRxS/T). This antibody is hereafter referred to anti-RRxS/T.

Consistent with our phosphoproteome analysis and as reported previously, we observed that MAF1 phosphorylation at PKA consensus sites was strongly reduced upon rapamycin treatment (Figure 2A). Although this could suggest that TORC1 activates PKA toward MAF1, this interpretation is complicated by the fact that the TORC1 effector SCH9, an AGC kinase family member like PKA, can also directly phosphorylate PKA sites in MAF1 (Huber *et al.,* 2009; Lee *et al.,* 2009). To further investigate whether TORC1 indeed activates PKA toward MAF1, we used the cell-permeable phosphodiesterase resistant analogue 8-Bromo-cAMP (Verma *et al.,* 1988) to activate PKA in the absence of TORC1 and SCH9 activity. As expected, PKA inactivation upon glucose starvation resulted in a strong reduction in MAF1 phosphorylation at PKA sites, and addition of 8-Br-cAMP to glucose-starved cells restored MAF1 phosphorylation at PKA sites (Figure 2B and Supplementary Figure 2A). Treatment of cells with 8-Br-cAMP also counteracted the inhibitory effect of rapamycin on the phosphorylation of MAF1 at PKA sites (Figure 2C and Supplementary Figure 2B). These data suggest that TORC1 indeed activates PKA (in addition to SCH9) toward MAF1.

We also examined phosphorylation of PKA sites in YPK3 and KSP1. YPK3 is an AGC kinase that is phosphorylated by PKA in vitro (Budovskaya *et al.,* 2005; Ptacek *et al.,* 2005). KSP1 is a serine/threonine kinase required during filamentous growth in response to nutrient limitation (Bharucha *et al.,* 2008). KSP1 localization is influenced by PKA, and it is also a PKA substrate in vitro (Ptacek *et al.,* 2005; Bharucha *et al.,* 2008). Similar to MAF1 and again consistent with our phosphoproteome analysis, phosphorylation of both KSP1 and YPK3 at consensus PKA site(s) decreased upon rapamycin treatment (Figure 2A). Similar to MAF1, but to a lesser extent, activation of PKA with 8-Br-cAMP counter-

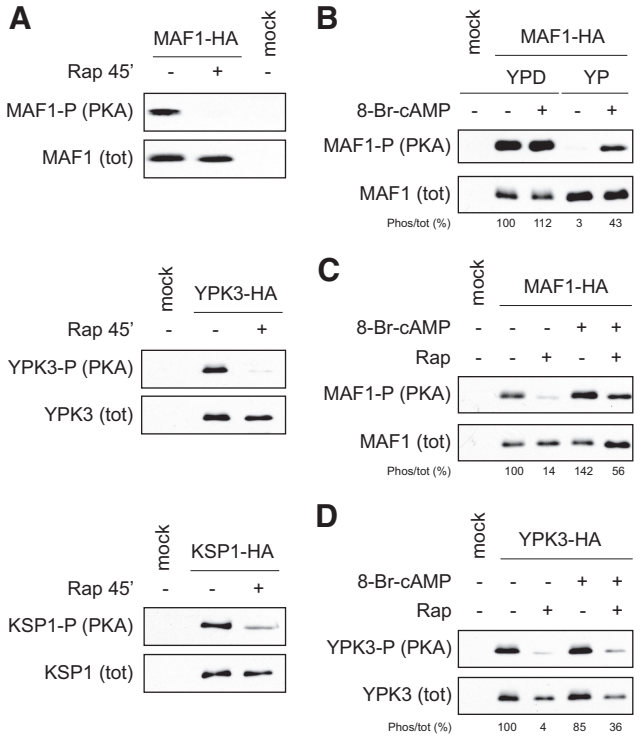

Figure 2. Influence of TORC1 inhibition on PKA substrate phosphorylation in vivo. (A) Rapamycin affects the phosphorylation state of different PKA substrates. Yeast strains expressing MAF1-HA (SA148), YPK3-HA (SA216), or KSP1-HA (SA219) were grown to exponential phase and treated for the indicated time with 200 ng/ml rapamycin (+) or drug vehicle (−). After protein extraction each tagged protein was immunoprecipitated and analyzed by Western blot for total protein (tot) with anti-HA antibody and for phosphorylation at PKA site (PKA) with anti-RRxS/T antibody. TB50a was used for mock control. (B) The yeast strain SA148 expressing MAF1-HA was grown to exponential phase in YPD and then shifted or not to YP for 2 h. Aliquots of cells were then treated for 30 min with 5 mM of 8-Br-cAMP. MAF1-HA was immunoprecipitated from total cell lysate and analyzed as described in A. TB50a was used as mock control. For each condition, the phosphorylation at PKA sites was quantified and normalized against the level of total protein and expressed as a percentage [Phos/tot (%)]. (C) The yeast strain SA148 expressing MAF1-HA was grown to exponential phase in YPD and then pretreated or not with 5 mM of 8-Br-cAMP during 5 min. Aliquots of cells were then treated for 30 min with 200 ng/ml rapamycin. Phosphorylation of MAF1-HA was analyzed as in A and B. TB50a was used for mock control. Phosphorylation was quantified as in B [Phos/tot (%)]. (D) The yeast strain SA216 expressing YPK3-HA was treated and analyzed as in C.

acted the inhibitory effect of rapamycin on the phosphorylation of YPK3 at PKA sites (Figure 2D). We did not examine the effect of 8-Br-cAMP on KSP1 for technical reasons. The above taken together indicates that MAF1, YPK3, and likely KSP1 are phosphorylated by PKA in a TORC1-dependent manner.

Type 2A and type 2A-like phosphatases are well-known downstream effectors of TORC1 and are activated upon TORC1 inactivation (Jiang and Broach, 1999; Jacinto *et al.*, 2001; Crespo and Hall, 2002). We have reported previously that the effect of TORC1 inhibition on several PKA-dependent processes is independent of both PP2A and the PP2A-like phosphatase SIT4 (Martin *et al.*, 2004; Schmelzle *et al.*, 2004). The above results with 8-Br-cAMP also suggest that the rapamycin-induced decrease in PKA target site phosphorylation is due to loss of PKA activity rather than to activation of a phosphatase.

We also used anti-RRxS/T to probe MSN2, CDC25, YAK1, and CKI1, all PKA substrates but whose PKA site phosphorylation was either not detected (CDC25, YAK1, and CKI1) or not altered in response to rapamycin (MSN2) in our phosphoproteome analysis. Probing with anti-RRxS/T detected all four proteins but failed to detect a change in their phosphorylation upon rapamycin treatment (see Supplementary Figure 3). Thus, large scale and targeted analyses of PKA site phosphorylation suggest that TORC1, rather than activating PKA globally, selectively activates PKA toward a subset of substrates.

BCY1 Is Highly Phosphorylated upon TORC1 Inactivation

To obtain insight into the molecular mechanism by which TORC1 might regulate PKA, we focused on BCY1. After confirming earlier observations that physiologically relevant TPK1–BCY1 interaction cannot be monitored in vitro or in vivo (Supplementary Figure 4 and data not shown), we examined BCY1 phosphorylation. As shown previously, BCY1 is highly phosphorylated upon glucose starvation, and this phosphorylation appears to be important for PKA nuclear localization, suggesting that BCY1 phosphorylation leads to BCY1 activation and PKA inactivation (Werner-Washburne *et al.*, 1991; Griffioen *et al.*, 2001). We observed that rapamycin treatment resulted in a slower migrating, phosphatase-sensitive form of BCY1 (Figure 3A), suggesting that TORC1 might signal to PKA via inhibition of BCY1 phosphorylation.

To investigate further whether TORC1 signals to PKA via BCY1 phosphorylation, we identified the phosphorylation sites in HA-tagged BCY1 isolated from rapamycin-treated and untreated cells (see *Materials and Methods*). In total, 17 phosphorylation sites were identified (Figure 3B and Supplementary Table 10). The 17 sites fell into three clusters, all in the N-terminal part of BCY1 (Figure 3B). The first cluster was S68, S70, S74, S77, S79, S81, S83, and S84. This cluster of phosphorylation sites, termed cluster II (CII), was described previously and was shown to be important for BCY1 function (Griffioen *et al.*, 2001). The second cluster of phosphorylated residues consisted of T144, S145, S147, T150, and T160. This cluster falls within or near the so-called autoinhibitory domain where the catalytic subunit of PKA "autophosphorylates" the highly conserved S145 (RRxS^{145}) to inhibit BCY1 (Kuret *et al.*, 1988; Werner-Washburne *et al.*, 1991). The third cluster of phosphorylated residues included T129, S130, and T131. This cluster was novel and was termed cluster III (CIII). We note that, in addition to the above 17 phosphorylation sites, we also detected phosphorylation in an extreme N-terminal, HA-containing fragment of BCY1, but were unable to pinpoint the phosphorylated residue(s) (data not shown). This phosphorylation is presumably related to the previously identified cluster I (CI; Griffioen *et al.*, 2001).

Consistent with the above observation that rapamycin treatment induced BCY1 phosphorylation as measured by altered electrophoretic mobility (Figure 3A), we detected more BCY1 phosphopeptides in extracts from rapamycin-treated cells compared with untreated cells. In particular, sites in CIII (and to a lesser extend in CII) were hyperphosphorylated in response to rapamycin (Supplementary Table 10). These results suggest that there are many TORC1-sensitive phosphorylation sites in BCY1, mainly in CIII. This may explain why previous studies, which did not examine rapamycin-treated cells, did not detect the phosphorylation sites in CIII.

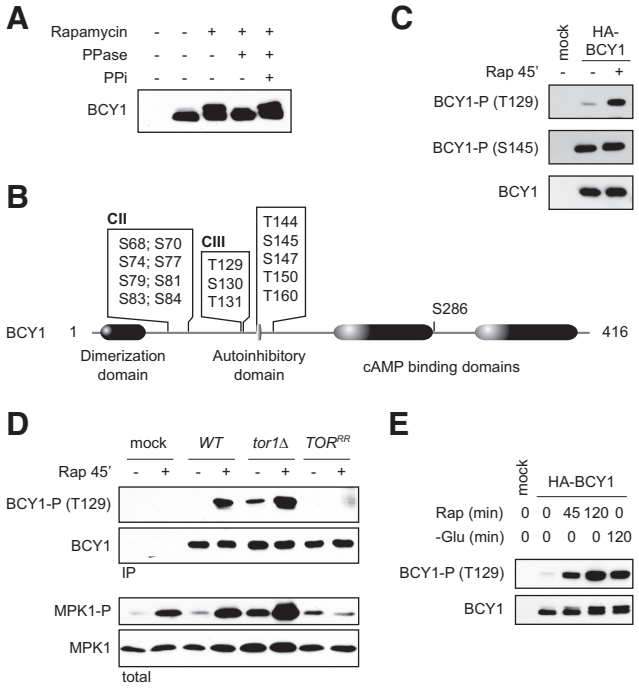

Figure 3. The PKA regulatory subunit BCY1 is highly phosphorylated upon TORC1 inhibition. (A) Exponentially growing cells expressing HA-BCY1 from a plasmid (SA094) or not (TB50a) were treated for 2 h with drug vehicle or rapamycin at 200 ng/ml. Total proteins were extracted and HA-BCY1 was immunoprecipitated. Aliquots of IPs belonging to the rapamycin treated samples were further treated with phosphatase (PPase) or not, in presence of phosphatase inhibitors (PPi) or not. BCY1 phosphorylation was observed by gel-shift assay followed by Western blotting with an anti-HA antibody. (B) Graphical representation of the phosphorylated amino acids identified in BCY1 by phosphopeptide enrichment and MS. CII/III, cluster II/III. (C) Similar to A except that yeast cells were treated with rapamycin for 45 min (Rap). Total BCY1 was followed by Western blot with anti-BCY1 (BCY1) antibody and the different phosphorylated form of BCY1 with anti-RRxS/T antibody [(BCY1-P (S145)] and anti-RxxS/T antibody [BCY1-P (T129)], respectively. (D) The procedure used in B was used to analyze rapamycin-induced phosphorylation of HA-BCY1 in wild-type (*WT* = TB50a), *TOR1* deletion (*tor1*Δ = AN9-2a), and rapamycin resistant TORs (*TOR*^{RR} = *TOR1-1 TOR2-1* = RL206-4D) yeast strain carrying pTS137 (panel IP). In parallel, total (MPK1) and activated MPK1 (MPK1-P) were visualized by Western blot on the total cell lysates used for the HA-BCY1 IPs (panel total). (E) Wild-type cells (*WT* = SA094) expressing HA-BCY1 (pTS137) were treated with 200 ng/ml rapamycin (Rap) or shifted to YP medium lacking glucose (−Glu) for the indicated time. Total (HA-BCY1) and phosphorylated BCY1 [BCY1-P (T129)] were followed as in D.

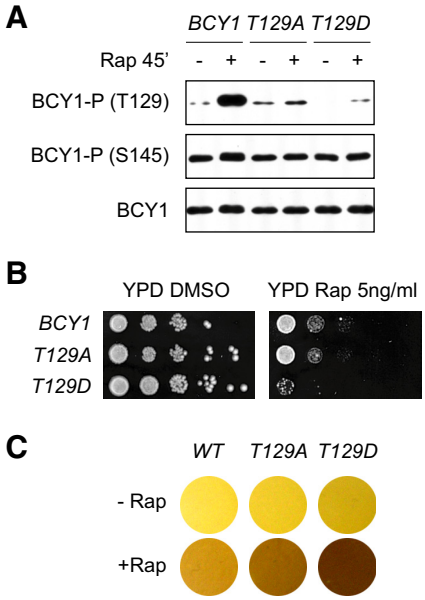

Figure 4. BCY1 T129 phosphorylation after rapamycin treatment lowers PKA activity. (A) The yeast strains expressing wild-type (WT) or different mutants of HA-BCY1 at threonine 129 (T129A, T129D) were grown to exponential phase and treated or not with rapamycin (200 ng/ml) for 45 min. After total protein extraction, HA-BCY1 was immunoprecipitated. Total BCY1 and phosphorylated BCY1 at S145 and T129 were detected by Western blot with the corresponding antibodies. (B) The yeast strains used in A were grown to exponential phase. A cell quantity corresponding to 1.0 $OD_{600\,nm}$ was serially 10-fold diluted and spotted on YPD plates containing DMSO or 5 ng/ml rapamycin. Plates were then incubated at 30°C for 3–5 d. (C) Glycogen accumulation was tested by iodine staining after 5-h rapamycin or drug vehicle treatment of yeast strains expressing the wild-type (*BCY1* = SA094) and mutated form of *BCY1* at threonine 129 (*T129A* and *T129D*).

S145 is part of an RRxS motif, whereas S74, S83, and T129 are part of RxxS/T sequences. To further characterize the rapamycin-induced phosphorylation sites in BCY1, we took advantage of two antibodies, the previously described anti-RRxS/T that specifically recognizes a phosphorylated PKA site (e.g., phosphorylated S145) and a second antibody (anti-RxxS/T) that recognizes the related, phosphorylated motif RxxS/T (e.g., phosphorylated T129). As described below and in supplementary information, the specificity of the two antibodies was confirmed by mutagenesis of their recognition sites in BCY1 (Figure 4A and Supplementary Figure 7). As shown in Figure 3C, HA-BCY1 immunoprecipitated with anti-HA was detected with both anti-RRxS/T and anti-RxxS/T. Although the signal obtained with anti-RRxS/T did not change significantly upon rapamycin treatment [Figure 3C, see P-BCY1 (S145)], the signal observed with anti-RxxS/T increased upon TORC1 inhibition [Figure 3C, see P-BCY1(T129)]. Thus, consistent with BCY1 phosphosite-mapping experiments described above, TORC1 inhibits phosphorylation of RxxS/T sites in BCY1 and has no effect on RRxS^{145} phosphorylation.

To confirm that the effect of rapamycin on BCY1 phosphorylation was indeed due to inhibition of TORC1, we examined BCY1 phosphorylation in *TOR* mutant strains. In a *TOR1* deletion strain, BCY1 was hyperphosphorylated at the RxxS/T site(s). Conversely, this site(s) remained insensitive to rapamycin in the rapamycin resistant (*TOR*^{RR}) *TOR1-1 TOR2-1* strain (Figure 3D). Thus, the effect of rapamycin on phosphorylation of BCY1 at the RxxS/T motif was due to TORC1 inhibition. Furthermore, phosphorylation of the RxxS/T motif in BCY1 increased with increasing time of rapamycin treatment, reaching a level after 2 h comparable to that of glucose starvation for 2 h (Figure 3E). Taken together, the above results suggest that TORC1 (and glucose) inhibits phosphorylation of multiple sites in BCY1, some if not all of which are part of an RxxS/T motif (e.g., S74, S83, and T129).

TORC1-sensitive BCY1 T129 Phosphorylation Inactivates PKA

To determine the effect of TORC1-sensitive BCY1 phosphorylation on PKA function, we mutated individually S74, S83,

and T129 to alanine or to phosphomimetic aspartate. Each mutant was then examined for rapamycin sensitivity and rapamycin-induced glycogen accumulation, two phenotypes that reflect PKA inactivity (Schmelzle *et al.*, 2004; Zurita-Martinez and Cardenas, 2005). We note that mutation of T129 reduced recognition by anti-RxxS/T, whereas mutation of S74 and S83 had no effect on recognition by this antibody (Figure 4A and data not shown). Thus, the region containing T129 was the main epitope in BCY1 recognized by anti-RxxS/T (Figure 4A). The phosphomimetic mutation *BCY1*^{T129D} conferred increased sensitivity to rapamycin and enhanced accumulation of glycogen upon TORC1 inhibition (Figure 4, B and C), suggesting that the BCY1^{T129D} protein is a constitutive inhibitor of PKA and that T129 phosphorylation activates BCY1 to inhibit PKA (at least toward some substrates). However, *BCY1*^{T129A} behaved like wild-type *BCY1*, as determined by rapamycin sensitivity and glycogen accumulation. Furthermore, mutation of T129 to alanine or aspartate did not affect nuclear localization of BCY1, rapamycin-dependent nuclear localization of TPK1, BCY1-TPK1 interaction, or PKA-dependent phosphorylation of MAF1 (data not shown). These results suggest that phosphorylation of a site(s) other than T129 can also activate BCY1. This other site is likely not S74, S83, or T131, as mutation of any one of these sites had no phenotypic consequence in our assays (data not shown). Taken together, our results suggest that TORC1 controls PKA (at least toward some substrates) by inhibiting phosphorylation of T129 and possibly other so far unknown sites in BCY1.

TORC1 Controls PKA via SCH9

As reported recently, TORC1 directly phosphorylates and activates the serine/threonine kinase and S6K homolog SCH9 (Urban *et al.*, 2007). Several reports have suggested that SCH9 is linked to PKA signaling. For example, the *SCH9* gene was initially identified as a multicopy suppressor of mutations that reduce PKA activity, and SCH9 prevents glycogen accumulation and activates ribosomal protein gene expression similar to PKA (Toda *et al.*, 1988; Urban *et al.*, 2007). To determine whether TORC1 controls BCY1 (and PKA) via SCH9, we examined BCY1 T129 phosphorylation in *SCH9*-deleted cells. As shown in Figure 5A, BCY1 was hyperphosphorylated at T129 in the *sch9* deletion mutant, even when TORC1 was active (absence of rapamycin). Consistent with this observation, PKA-dependent phosphorylation of MAF1 was decreased in the *sch9* mutant (Figure 5B). Cells deleted for *SCH9* also displayed constitutive nuclear localization of the catalytic subunit TPK1 (Figure 5C). *sch9*^{5A} mutant cells, in which all residues required for SCH9 phosphorylation and activation by TORC1 are mutated to alanine, also displayed constitutive nuclear accumulation of TPK1 (Figure 5C). Furthermore, in normal growth conditions, *sch9* deletion and *sch9*^{5A} mutants displayed constitutive nuclear accumulation of the PKA target YAK1, similar to what is observed in wild-type cells treated with rapamycin (data not shown and Schmelzle *et al.*, 2004). Together, these observations suggest that TORC1 inhibits BCY1 T129 phosphorylation and TPK1 nuclear accumulation through SCH9.

The MAP Kinase MPK1 Directly Phosphorylates BCY1 upon TORC1 Inhibition

The results described above suggested that, upon TORC1 inhibition, BCY1 is phosphorylated on T129 and thereby activated. What is the T129 kinase that is inhibited by TORC1? Two serine/threonine kinases, YAK1 and MCK1, have been shown to mediate BCY1 phosphorylation upon

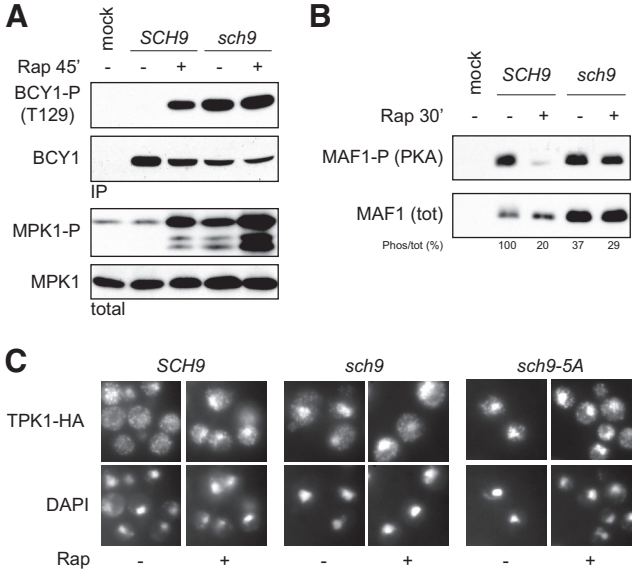

Figure 5. TORC1 inhibits MPK1 and BCY1 T129 phosphorylation through the AGC kinase SCH9. (A) To follow the influence of SCH9 on BCY1 T129 and MPK1 phosphorylation, the yeast strains SA094 (*WT*) and SA135 (*sch9*) expressing HA-BCY1 were grown to exponential phase and treated 45 min with rapamycin (+) or drug vehicle (−) before total protein extraction. HA-BCY1 was immunoprecipitated (IP) and analyzed by Western blot with anti-HA (HA-BCY1) and anti-RxxS/T [BCY1-P (T129)] antibodies (IP panel). Total (MPK1) and activated MPK1 (MPK1-P) were visualized in total cell lysate by Western blot with the corresponding antibodies (panel total). (B) Effect of *SCH9* deletion on PKA-dependent phosphorylation of MAF1. The yeast strains SA148 (*MAF1-HA SCH9*) and SA232 (*MAF1-HA sch9*) were grown to exponential phase and treated for 30 min with rapamycin (+) or drug vehicle (−) before total protein extraction. MAF1-HA was immunoprecipitated and analyzed by Western blot with anti-HA [MAF1 (tot)] and anti-RRxS/T [MAF1-P (PKA)] antibodies. For each condition, the phosphorylation at PKA sites was quantified, normalized against the level of total protein, and expressed as percentage [Phos/tot (%)]. (C) The rapamycin-dependent localization of TPK1-HA (TPK1) was followed by immunofluorescence of yeast strain SA20X carrying a plasmid expressing wild-type *SCH9* (*WT* = pJU675), no *SCH9* (*sch9* = pRS416), or the mutant *sch9-*^{5A} (*sch9-5A* = pJU822). Cells were treated 30 min with rapamycin (+) or drug vehicle (−). TPK1-HA was localized by the use of an anti-HA antibody. The nucleus was observed by DAPI staining (DNA).

nutrient limitation or other stress (Werner-Washburne *et al.*, 1991; Griffioen *et al.*, 2001). YAK1 is activated upon TORC1 inhibition and antagonizes the PKA pathway (Zappacosta *et al.*, 2002; Martin *et al.*, 2004; Deminoff *et al.*, 2006). MCK1 is a glycogen synthase kinase 3 (GSK3) homologue involved in meiosis (Neigeborn and Mitchell, 1991; Kassir *et al.*, 2006). In mutants deleted for *YAK1* or *MCK1*, rapamycin-induced phosphorylation of BCY1 T129 was reduced but not abolished (Supplementary Figures 5, A and B). In addition, YAK1 and MCK1 purified from rapamycin-treated or -untreated yeast cells failed to phosphorylate recombinant GST-BCY1 in vitro (data not shown). These findings suggest that YAK1 and MCK1 may affect BCY1 phosphorylation but are not the kinases that directly phosphorylate BCY1 T129 upon TORC1 inhibition.

Next, we examined BCY1 T129 phosphorylation in cells lacking either NPR1 or SLT2/MPK1, two serine/threonine kinases that are activated upon TORC1 inhibition (Schmidt *et al.*, 1998; Krause and Gray, 2002; Torres *et al.*, 2002). NPR1 controls the sorting of several amino acid transporters in

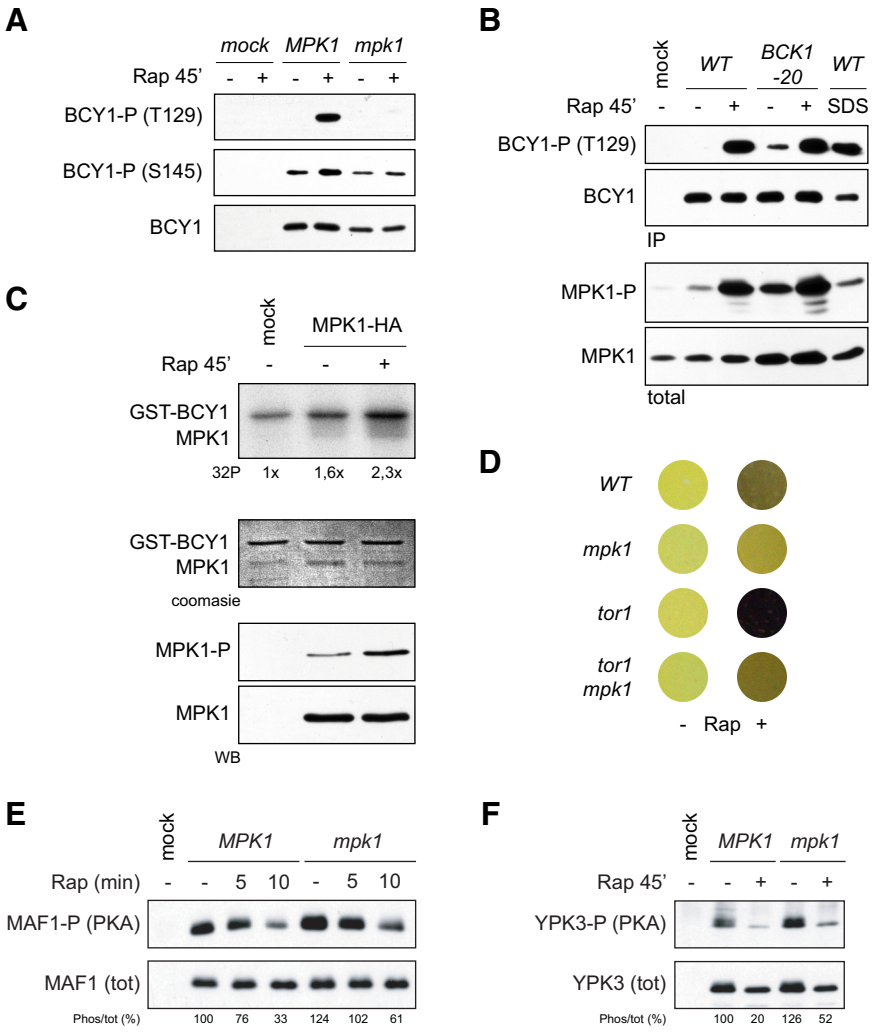

Figure 6. BCY1 T129 phosphorylation is mediated by activation of the MAP kinase MPK1. (A) Yeast strains wild type (*MPK1* = TB50a) or deleted (*mpk1* = TS45-1a) for MPK1 and expressing HA-BCY1 from a plasmid (pTS137) were treated for 45 min with 200 ng/ml rapamycin (+) or drug vehicle (−). After protein extraction, HA-BCY1 was immunoprecipitated and analyzed by Western blot using anti-HA (HA-BCY1), anti-RRxS/T [BCY1-P (S145)], and anti-RxxS/T (BCY1-P (T129)) antibodies. TB50a was used as a mock control. (B) Total (HA-BCY1) and phospho-T129 BCY1 [BCY1-P (T129)] were analyzed as in A after 45-min treatment with rapamycin (200 ng/ml), SDS (0.01%), or drug vehicle of wild-type strain (*WT* = TB50a) or of a strain expressing an hyperactive form of BCK1 (*BCK1-20*) from a plasmid (pRS316::BCK1-20; panel IP). In parallel, total MPK1 (MPK1) and active phosphorylated MPK1 (P-MPK1) were analyzed by Western blot on the total extracts used for HA-BCY1 IPs with the corresponding antibodies (panel total). (C) In vitro kinase assay. MPK1-HA was immunoprecipitated from the yeast strain TS99-5c treated with rapamycin (+) or drug vehicle (−) for 45 min. The assay was performed as describe in *Materials and Methods* in presence of 1 μg of recombinant GST-BCY1 expressed from *E. coli*. Total and phosphorylated proteins were visualized by Coomassie staining (Coomassie) and autoradiography (32P), respectively. An aliquot of purified MPK1-HA was conserved for analysis of total (MPK1) and activated MPK1 (MPK1-P) by Western blot as above (WB). The level of BCY1 phosphorylation was quantified by densitometric analysis (below panel 32P). MBP, a commonly used MPK1 in vitro substrate, was used as a positive control (data not shown) (D) Glycogen accumulation was tested by iodine staining after 5-h rapamycin or drug vehicle treatment of yeast strains wild type (*WT* = SA180) or deleted for *MPK1* (*mpk1* = SA183), for *TOR1* (*tor1* = SA181), or for both genes (*tor1 mpk1* = SA185). (E) Effect of *MPK1* deletion on PKA-dependent phosphorylation of MAF1. Yeast strains containing MAF1-HA and expressing (*MPK1*; strain SA148) or lacking MPK1 (*mpk1*; strain SA233) were grown to exponential phase and treated for the indicated time with rapamycin or drug vehicle before total protein extraction. MAF1-HA was immunoprecipitated and analyzed by Western blot with anti-HA [MAF1 (tot)] and anti-RRxS/T (MAF1-P (PKA)) antibodies. MAF1 phosphorylation at PKA sites was quantified as described in Figure 1 [Phos/tot (%)]. (F) Effect of *MPK1* deletion on PKA-dependent phosphorylation of YPK3. Yeast strains containing YPK3-HA and expressing (*MPK1*; strain SA234) or lacking MPK1 (*mpk*1; SA235) were analyzed as in E except that the cells were treated with rapamycin (+) or drug vehicle (−) for 45 min.

response to nutrients (Schmidt *et al.*, 1998). Deletion of *NPR1* had no effect on T129 phosphorylation upon rapamycin treatment (Supplementary Figure 5C). The MAP kinase MPK1 is part of the PKC1-BCK1-MKK1/2-MPK1 cascade that regulates cell wall integrity and entry into quiescence in response to stress (Levin, 2005). Deletion of *MPK1* completely abolished rapamycin-induced T129 phosphorylation (Figure 6A). To further investigate a role of MPK1 in BCY1 phosphorylation, we examined T129 phosphorylation in response to conditions that activate the cell wall integrity pathway. We activated the cell wall integrity pathway with a genetically activated MAPKKK (*BCK1-20* mutation) or with chemicals such as SDS, Congo Red, and sodium orthovanadate that disrupt the cell wall. MPK1 activation was monitored with an antibody that recognizes phosphorylated p44/42 ERK MAPK but that also recognizes phosphorylated MPK1 in yeast (Verna *et al.*, 1997; Delley and Hall, 1999). Like rapamycin treatment (Krause and Gray, 2002; Torres *et al.*, 2002 and Figure 6B), activation of the cell wall integrity pathway stimulated both MPK1 and BCY1 T129 phosphorylation (Figure 6B and Supplementary Figure 6C). We next examined whether MPK1 immunopurified from rapamycin-treated cells phosphorylates recombinant BCY1 in vitro. As shown in Figure 6C, MPK1 purified from rapamycin-treated cells indeed phosphorylated recombinant BCY1. Recombinant BCY1 in which T129 was mutated to alanine was less phosphorylated compared with wild-type BCY1 (Supplementary Figure 6E). These results suggest that MPK1 directly phosphorylates BCY1 T129 upon TORC1 inhibition in vivo.

To investigate the physiological significance of MPK1-dependent BCY1 phosphorylation upon TORC1 inhibition, we examined rapamycin-induced glycogen accumulation and PKA-dependent phosphorylation of MAF1 and YPK3 in cells lacking MPK1. Rapamycin-treated, *MPK1*-deleted cells accumulated less glycogen than wild-type cells (Figure 6D). A role for MPK1 in TORC1-sensitive glycogen accumulation

was confirmed by the observation that *MPK1* deletion abolished the hyperaccumulation of glycogen provoked by a *TOR1* deletion (Figure 6D). Conversely, and similar to rapamycin treatment, activation of the cell wall integrity pathway by SDS or caffeine (Levin, 2005) stimulated glycogen accumulation (Supplementary Figure 6D). Furthermore, in *MPK1*-deleted cells, phosphorylation of PKA sites in MAF1 and YPK3 was increased and rapamycin-induced dephosphorylation of these sites was reduced (Figure 6, E and F). Thus, MPK1 appears to have a physiological role in TORC1-mediated control of PKA.

Is SCH9 upstream of MPK1 in controlling phosphorylation of BCY1 T129, as expected from the above findings? MPK1 was hyperphosphorylated in *sch9* deletion and $sch9^{5A}$ mutants, even when TORC1 was active (absence of rapamycin; Figure 5A and Supplementary Figure 6A). Furthermore, *sch9* deletion mutants displayed enhanced resistance to zymolyase, a cell wall–damaging agent (Supplementary Figure 6B), suggesting that the cell wall integrity pathway was hyperactive in cells lacking SCH9. Thus, SCH9 appears to negatively control both BCY1 T129 phosphorylation and MPK1 activity, suggesting that SCH9 is indeed upstream of MPK1 in controlling BCY1 T129 phosphorylation. The above results taken together suggest that TORC1-SCH9 signaling activates PKA (at least toward some substrates) by inhibiting MPK1 direct phosphorylation of BCY1 T129.

DISCUSSION

To obtain insight into the shared regulation by PKA and TORC1 (see *Introduction*), we investigated the TORC1 phosphoproteome. This revealed that PKA phosphorylation sites are a primary target of TORC1, suggesting that TORC1 is an upstream activator of PKA. However, many PKA sites were not affected by TORC1, suggesting that TORC1 activates PKA selectively rather than globally (see below). Thus, both models that account for the shared regulation by TORC1 and PKA appear to be valid. First, TORC1 is an upstream regulator of PKA toward some substrates, such as MAF1, YPK3, and KSP1, whose phosphorylation by PKA is TORC1-dependent. Second, TORC1 and PKA are in distinct but parallel pathways that converge on common target proteins or processes. This latter case includes proteins whose phosphorylation by PKA is not TORC1 dependent.

To investigate the molecular mechanism by which TORC1 controls PKA, we focused on the PKA negative regulatory subunit BCY1. We found that TORC1 inhibits phosphorylation of T129 (and other sites) in BCY1. Phenotypes conferred by mutation of T129 to phosphomimetic aspartate suggest that T129 phosphorylation activates BCY1 and thereby inactivates PKA. Furthermore, we found that TORC1 inhibits BCY1 T129 phosphorylation by inhibiting the MAP kinase MPK1. TORC1 inhibits MPK1 via the S6K ortholog SCH9. Thus, we have defined a pathway, consisting of TORC1-SCH9-MPK1-BCY1-PKA, by which TORC1 prevents inactivation of PKA. Although TORC1 phoshorylates and activates SCH9 directly and MPK1 phosphorylates (T129) and activates BCY1 directly, it remains to be determined how SCH9 inhibits phosphorylation and activation of MPK1 (see below).

How could regulation of BCY1 by TORC1 control PKA activity toward some but not all PKA substrates? On rapamycin treatment, BCY1 sequesters PKA in the nucleus (Schmelzle *et al.,* 2004). This and our above findings suggest that phosphorylated BCY1 (at T129 and likely other sites) maintains PKA in the nucleus upon TORC1 inhibition and may thus control access of PKA to specific substrates. This control of PKA by BCY1 phosphorylation would be independent of PKA control by binding of cAMP to BCY1. This model is also supported by our observation that any mutation that disrupts the BCY1-TPK1 interaction, e.g., $BCY1^{S145D}$ or $TPK1^{T241A/D/E}$, prevents nuclear accumulation of TPK1 upon rapamycin treatment (Supplementary Figure 7 and data not shown). Finally, this model is similar to a model proposed by Griffioen *et al.* (2001, 2003), suggesting that BCY1 phosphorylation upon glucose limitation controls PKA localization and accessibility to substrates. An alternative model is that T129-phosphorylated BCY1 binds and inhibits only a specific pool of PKA. This separate pool of PKA could be due to differential modification or localization of PKA by unknown factors. Different pools of PKA might be in part explained by the fact that there are three catalytic subunits of PKA (TPK1, TPK2, and TPK3) in yeast. Confirmation of the above or other possible models will require further study.

Griffioen *et al.* (2001, 2003) showed that BCY1 is phosphorylated on two clusters of serines (CI and CII) in response to stress. Here we identified, in addition to CI and CII, a third cluster of serine and threonine residues (CIII) that are phosphorylated upon rapamycin treatment. T129 in CIII is an important residue in the regulation of BCY1 and ultimately PKA. However, the mild phenotypes conferred by mutation of T129 to alanine or aspartate suggest that phosphorylation at this residue is not the sole event regulating BCY1 and PKA upon TORC1 inhibition. BCY1 is phosphorylated on at least 16 serine or threonine residues other than T129, including S74, S79, S83, T131, and S145. However, individual mutation of S74, S79, and S83 and T131 had no phenotypic consequence (data not shown). A phosphomimetic mutation of S145 resulted in BCY1 inactivation, suggesting that phosphorylation of this site regulates BCY1, but the phosphorylation of S145 was independent of TORC1 (Supplementary Figure 7). Further study will be required to determine the roles and kinase(s) for all the phosphorylation sites in BCY1.

MPK1 is a MAP kinase in the PKC1/cell wall integrity pathway that is activated in response to several stresses including TORC1 inhibition (Krause and Gray, 2002; Torres *et al.,* 2002; Levin, 2005). Earlier studies have reported genetic interactions between the cell wall integrity pathway and the PKA pathway. For example, activation of the cell wall integrity pathway suppresses the heat-shock sensitivity caused by hyperactive RAS-cAMP signaling, and the RHO1 GDP/GTP exchange factor ROM2, which acts early in the cell integrity pathway, is required for PKA-mediated stress response (Verna *et al.,* 1997; Park *et al.,* 2005; Kuranda *et al.,* 2006). Our observation that MPK1 phosphorylates and activates BCY1 is consistent with the above genetic interactions. Finally, we note that MPK1 is likely not the only kinase involved in PKA regulation by TORC1, as rapamycin-induced nuclear accumulation of PKA is not altered by loss of MPK1 (whereas BCY1 phosphorylation is) or presence of BCK1-20, a hyperactive MAPKKK BCK1 upstream of MPK1 (data not shown). Furthermore *MPK1* deletion reduces but does not abolish rapamycin-induced dephosphorylation of MAF1 and YPK3.

TORC1 directly phosphorylates and activates the protein kinase SCH9 (Urban *et al.,* 2007). SCH9 was originally identified as a multicopy suppressor of a PKA defect (Toda *et al.,* 1988). Furthermore, *SCH9* deletion severely decreases PKA-dependent phosphorylation of MSN2 and MAF1 (Trott *et al.,* 2005; Huber *et al.,* 2009; Lee *et al.,* 2009). In agreement with these previous observations, we find that SCH9 acts downstream of TORC1 to maintain MPK1 inactive and PKA active. The molecular link between SCH9 and MPK1 is likely

indirect because MPK1 is phosphorylated and active when SCH9 is inactive. The link between SCH9 and MPK1 may involve ROM2. ROM2 was recently shown to interact genetically with the TORC1, PKA, and cell wall integrity pathways (Park *et al.*, 2005; Kuranda *et al.*, 2006).

ACKNOWLEDGMENTS

We thank J. M. Thevelein (University of Leuven, Belgium) for plasmids, R. Loewith (University of Geneva, Switzerland) for yeast strains and discussions, and D. Schwartz for the kind advice on using Motif-X 1.2. This work was supported by grants from the Canton of Basel, SystemsX.ch and the Swiss National Science Foundation (M.N.H).

REFERENCES

Aronova, S., Wedaman, K., Aronov, P. A., Fontes, K., Ramos, K., Hammock, B. D., and Powers, T. (2008). Regulation of ceramide biosynthesis by TOR complex 2. Cell Metab. *7*, 148–158.

Barbet, N. C., Schneider, U., Helliwell, S. B., Stansfield, I., Tuite, M. F., and Hall, M. N. (1996). TOR controls translation initiation and early G1 progression in yeast. Mol. Biol. Cell *7*, 25–42.

Beck, T., and Hall, M. N. (1999). The TOR signalling pathway controls nuclear localization of nutrient-regulated transcription factors. Nature *402*, 689–692.

Bharucha, N., Ma, J., Dobry, C. J., Lawson, S. K., Yang, Z., and Kumar, A. (2008). Analysis of the yeast kinome reveals a network of regulated protein localization during filamentous growth. Mol. Biol. Cell *19*, 2708–2717.

Budovskaya, Y. V., Stephan, J. S., Deminoff, S. J., and Herman, P. K. (2005). An evolutionary proteomics approach identifies substrates of the cAMP-dependent protein kinase. Proc. Natl. Acad. Sci. USA. *102*, 13933–13938.

Cannon, J. F., and Tatchell, K. (1987). Characterization of *Saccharomyces cerevisiae* genes encoding subunits of cyclic AMP-dependent protein kinase. Mol. Cell. Biol. *7*, 2653–2663.

Cox, J., and Mann, M. (2008). MaxQuant enables high peptide identification rates, individualized p.p.b.-range mass accuracies and proteome-wide protein quantification. Nat. Biotechnol. *26*, 1367–1372.

Cox, J., Matic, I., Hilger, M., Nagaraj, N., Selbach, M., Olsen, J. V., and Mann, M. (2009). A practical guide to the MaxQuant computational platform for SILAC-based quantitative proteomics. Nat. Protoc. *4*, 698–705.

Crespo, J. L., and Hall, M. N. (2002). Elucidating TOR signaling and rapamycin action: lessons from *Saccharomyces cerevisiae*. Microbiol. Mol. Biol. Rev. *66*, 579–591, table of contents.

Cybulski, N., and Hall, M. N. (2009). TOR complex 2, a signaling pathway of its own. Trends Biochem. Sci. *34*, 620–627.

De Virgilio, C., and Loewith, R. (2006). Cell growth control: little eukaryotes make big contributions. Oncogene *25*, 6392–6415.

Delley, P. A., and Hall, M. N. (1999). Cell wall stress depolarizes cell growth via hyperactivation of RHO1. J. Cell Biol. *147*, 163–174.

Deminoff, S. J., Howard, S. C., Hester, A., Warner, S., and Herman, P. K. (2006). Using substrate-binding variants of the cAMP-dependent protein kinase to identify novel targets and a kinase domain important for substrate interactions in *Saccharomyces cerevisiae*. Genetics *173*, 1909–1917.

Ghaemmaghami, S., Huh, W. K., Bower, K., Howson, R. W., Belle, A., Dephoure, N., O'Shea, E. K., and Weissman, J. S. (2003). Global analysis of protein expression in yeast. Nature *425*, 737–741.

Gorner, W., Durchschlag, E., Martinez-Pastor, M. T., Estruch, F., Ammerer, G., Hamilton, B., Ruis, H., and Schuller, C. (1998). Nuclear localization of the C2H2 zinc finger protein Msn2p is regulated by stress and protein kinase A activity. Genes Dev. *12*, 586–597.

Griffioen, G., Anghileri, P., Imre, E., Baroni, M. D., and Ruis, H. (2000). Nutritional control of nucleocytoplasmic localization of cAMP-dependent protein kinase catalytic and regulatory subunits in *Saccharomyces cerevisiae*. J. Biol. Chem. *275*, 1449–1456.

Griffioen, G., Branduardi, P., Ballarini, A., Anghileri, P., Norbeck, J., Baroni, M. D., and Ruis, H. (2001). Nucleocytoplasmic distribution of budding yeast protein kinase A regulatory subunit Bcy1 requires Zds1 and is regulated by Yak1-dependent phosphorylation of its targeting domain. Mol. Cell. Biol. *21*, 511–523.

Griffioen, G., Swinnen, S., and Thevelein, J. M. (2003). Feedback inhibition on cell wall integrity signaling by Zds1 involves Gsk3 phosphorylation of a cAMP-dependent protein kinase regulatory subunit. J. Biol. Chem. *278*, 23460–23471.

Gruhler, A., Olsen, J. V., Mohammed, S., Mortensen, P., Faergeman, N. J., Mann, M., and Jensen, O. N. (2005). Quantitative phosphoproteomics applied to the yeast pheromone signaling pathway. Mol. Cell Proteom. *4*, 310–327.

Guthrie, C., and Fink, G. R. (1991). Guide to Yeast Genetics and Molecular Biology, San Diego: Academic Press.

Hilger, M., Bonaldi, T., Gnad, F., and Mann, M. (2009). Systems-wide analysis of a phosphatase knock-down by quantitative proteomics and phosphoproteomics. Mol. Cell Proteom. *8*, 1908–1920.

Hill, J., Donald, K. A., and Griffiths, D. E. (1991). DMSO-enhanced whole cell yeast transformation. Nucleic Acids Res. *19*, 5791.

Ho, H. L., Shiau, Y. S., and Chen, M. Y. (2005). *Saccharomyces cerevisiae*TSC11/AVO3 participates in regulating cell integrity and functionally interacts with components of the Tor2 complex. Curr. Genet. *47*, 273–288.

Huber, A., Bodenmiller, B., Uotila, A., Stahl, M., Wanka, S., Gerrits, B., Aebersold, R., and Loewith, R. (2009). Characterization of the rapamycin-sensitive phosphoproteome reveals that Sch9 is a central coordinator of protein synthesis. Genes Dev. *23*, 1929–1943.

Jacinto, E., Guo, B., Arndt, K. T., Schmelzle, T., and Hall, M. N. (2001). TIP41 interacts with TAP42 and negatively regulates the TOR signaling pathway. Mol. Cell *8*, 1017–1026.

Jiang, Y., and Broach, J. R. (1999). Tor proteins and protein phosphatase 2A reciprocally regulate Tap42 in controlling cell growth in yeast. EMBO J. *18*, 2782–2792.

Johnson, K. E., Cameron, S., Toda, T., Wigler, M., and Zoller, M. J. (1987). Expression in *Escherichia coli* of BCY1, the regulatory subunit of cyclic AMP-dependent protein kinase from *Saccharomyces cerevisiae*. Purification and characterization. J. Biol. Chem. *262*, 8636–8642.

Jorgensen, P., Rupes, I., Sharom, J. R., Schneper, L., Broach, J. R., and Tyers, M. (2004). A dynamic transcriptional network communicates growth potential to ribosome synthesis and critical cell size. Genes Dev. *18*, 2491–2505.

Kaeberlein, M., Powers, R. W., 3rd, Steffen, K. K., Westman, E. A., Hu, D., Dang, N., Kerr, E. O., Kirkland, K. T., Fields, S., and Kennedy, B. K. (2005). Regulation of yeast replicative life span by TOR and Sch9 in response to nutrients. Science *310*, 1193–1196.

Kassir, Y., Rubin-Bejerano, I., and Mandel-Gutfreund, Y. (2006). The *Saccharomyces cerevisiae* GSK-3 beta homologs. Curr. Drug Targets *7*, 1455–1465.

Krause, S. A., and Gray, J. V. (2002). The protein kinase C pathway is required for viability in quiescence in *Saccharomyces cerevisiae*. Curr. Biol. *12*, 588–593.

Kuranda, K., Leberre, V., Sokol, S., Palamarczyk, G., and Francois, J. (2006). Investigating the caffeine effects in the yeast *Saccharomyces cerevisiae* brings new insights into the connection between TOR, PKC and Ras/cAMP signalling pathways. Mol. Microbiol. *61*, 1147–1166.

Kuret, J., Johnson, K. E., Nicolette, C., and Zoller, M. J. (1988). Mutagenesis of the regulatory subunit of yeast cAMP-dependent protein kinase. Isolation of site-directed mutants with altered binding affinity for catalytic subunit. J. Biol. Chem. *263*, 9149–9154.

Lee, J., Moir, R. D., and Willis, I. M. (2009). Regulation of RNA polymerase III transcription involves SCH9-dependent and SCH9-independent branches of the target of rapamycin (TOR) pathway. J. Biol. Chem. *284*, 12604–12608.

Levin, D. E. (2005). Cell wall integrity signaling in *Saccharomyces cerevisiae*. Microbiol. Mol. Biol. Rev. *69*, 262–291.

Li, X., Gerber, S. A., Rudner, A. D., Beausoleil, S. A., Haas, W., Villen, J., Elias, J. E., and Gygi, S. P. (2007). Large-scale phosphorylation analysis of alpha-factor-arrested *Saccharomyces cerevisiae*. J. Proteome Res. *6*, 1190–1197.

Loewith, R., Jacinto, E., Wullschleger, S., Lorberg, A., Crespo, J. L., Bonenfant, D., Oppliger, W., Jenoe, P., and Hall, M. N. (2002). Two TOR complexes, only one of which is rapamycin sensitive, have distinct roles in cell growth control. Mol. Cell *10*, 457–468.

Marion, R. M., Regev, A., Segal, E., Barash, Y., Koller, D., Friedman, N., and O'Shea, E. K. (2004). Sfp1 is a stress- and nutrient-sensitive regulator of ribosomal protein gene expression. Proc. Natl. Acad. Sci. USA *101*, 14315–14322.

Martin, D. E., Soulard, A., and Hall, M. N. (2004). TOR regulates ribosomal protein gene expression via PKA and the Forkhead transcription factor FHL1. Cell *119*, 969–979.

Moir, R. D., Lee, J., Haeusler, R. A., Desai, N., Engelke, D. R., and Willis, I. M. (2006). Protein kinase A regulates RNA polymerase III transcription through the nuclear localization of Maf1. Proc. Natl. Acad. Sci. USA *103*, 15044–15049.

Neigeborn, L., and Mitchell, A. P. (1991). The yeast MCK1 gene encodes a protein kinase homolog that activates early meiotic gene expression. Genes Dev. *5*, 533–548.

Olsen, J. V., de Godoy, L. M., Li, G., Macek, B., Mortensen, P., Pesch, R., Makarov, A., Lange, O., Horning, S., and Mann, M. (2005). Parts per million mass accuracy on an Orbitrap mass spectrometer via lock mass injection into a C-trap. Mol. Cell Proteom. *4*, 2010–2021.

Ong, S. E., Blagoev, B., Kratchmarova, I., Kristensen, D. B., Steen, H., Pandey, A., and Mann, M. (2002). Stable isotope labeling by amino acids in cell culture, SILAC, as a simple and accurate approach to expression proteomics. Mol. Cell Proteom. *1*, 376–386.

Park, J. I., Collinson, E. J., Grant, C. M., and Dawes, I. W. (2005). Rom2p, the Rho1 GTP/GDP exchange factor of *Saccharomyces cerevisiae*, can mediate stress responses via the Ras-cAMP pathway. J. Biol. Chem. *280*, 2529–2535.

Perkins, D. N., Pappin, D. J., Creasy, D. M., and Cottrell, J. S. (1999). Probability-based protein identification by searching sequence databases using mass spectrometry data. Electrophoresis *20*, 3551–3567.

Ptacek, J., *et al*. (2005). Global analysis of protein phosphorylation in yeast. Nature *438*, 679–684.

Reinke, A., Anderson, S., McCaffery, J. M., Yates, J., 3rd, Aronova, S., Chu, S., Fairclough, S., Iverson, C., Wedaman, K. P., and Powers, T. (2004). TOR complex 1 includes a novel component, Tco89p (YPL180w), and cooperates with Ssd1p to maintain cellular integrity in *Saccharomyces cerevisiae*. J. Biol. Chem. *279*, 14752–14762.

Santangelo, G. M. (2006). Glucose signaling in *Saccharomyces cerevisiae*. Microbiol. Mol. Biol. Rev. *70*, 253–282.

Santhanam, A., Hartley, A., Duvel, K., Broach, J. R., and Garrett, S. (2004). PP2A phosphatase activity is required for stress and Tor kinase regulation of yeast stress response factor Msn2p. Eukaryot. Cell *3*, 1261–1271.

Schawalder, S. B., Kabani, M., Howald, I., Choudhury, U., Werner, M., and Shore, D. (2004). Growth-regulated recruitment of the essential yeast ribosomal protein gene activator Ifh1. Nature *432*, 1058–1061.

Schmelzle, T., Beck, T., Martin, D. E., and Hall, M. N. (2004). Activation of the RAS/cyclic AMP pathway suppresses a TOR deficiency in yeast. Mol. Cell. Biol. *24*, 338–351.

Schmidt, A., Beck, T., Koller, A., Kunz, J., and Hall, M. N. (1998). The TOR nutrient signalling pathway phosphorylates NPR1 and inhibits turnover of the tryptophan permease. EMBO J. *17*, 6924–6931.

Schwartz, D., and Gygi, S. P. (2005). An iterative statistical approach to the identification of protein phosphorylation motifs from large-scale data sets. Nat. Biotechnol. *23*, 1391–1398.

Shabb, J. B. (2001). Physiological substrates of cAMP-dependent protein kinase. Chem. Rev. *101*, 2381–2411.

Soulard, A., Cohen, A., and Hall, M. N. (2009). TOR signaling in invertebrates. Curr. Opin. Cell Biol. *21*, 825–836.

Stephan, J. S., Yeh, Y. Y., Ramachandran, V., Deminoff, S. J., and Herman, P. K. (2009). The Tor and PKA signaling pathways independently target the Atg1/Atg13 protein kinase complex to control autophagy. Proc. Natl. Acad. Sci. USA *106*, 17049–17054.

Thingholm, T. E., Jorgensen, T. J., Jensen, O. N., and Larsen, M. R. (2006). Highly selective enrichment of phosphorylated peptides using titanium dioxide. Nat. Protoc. *1*, 1929–1935.

Toda, T., Cameron, S., Sass, P., and Wigler, M. (1988). SCH9, a gene of *Saccharomyces cerevisiae* that encodes a protein distinct from, but functionally and structurally related to, cAMP-dependent protein kinase catalytic subunits. Genes Dev. *2*, 517–527.

Toda, T., Cameron, S., Sass, P., Zoller, M., Scott, J. D., McMullen, B., Hurwitz, M., Krebs, E. G., and Wigler, M. (1987a). Cloning and characterization of BCY1, a locus encoding a regulatory subunit of the cyclic AMP-dependent protein kinase in *Saccharomyces cerevisiae*. Mol. Cell. Biol. *7*, 1371–1377.

Toda, T., Cameron, S., Sass, P., Zoller, M., and Wigler, M. (1987b). Three different genes in *S. cerevisiae* encode the catalytic subunits of the cAMP-dependent protein kinase. Cell *50*, 277–287.

Torres, J., Di Como, C. J., Herrero, E., and De La Torre-Ruiz, M. A. (2002). Regulation of the cell integrity pathway by rapamycin-sensitive TOR function in budding yeast. J. Biol. Chem. *277*, 43495–43504.

Trott, A., Shaner, L., and Morano, K. A. (2005). The molecular chaperone Sse1 and the growth control protein kinase Sch9 collaborate to regulate protein kinase A activity in *Saccharomyces cerevisiae*. Genetics *170*, 1009–1021.

Urban, J., *et al*. (2007). Sch9 is a major target of TORC1 in *Saccharomyces cerevisiae*. Mol. Cell *26*, 663–674.

Verma, R., Iida, H., and Pardee, A. B. (1988). Modulation of expression of the stress-inducible p118 of *Saccharomyces cerevisiae* by cAMP. II. A study of p118 expression in mutants of the cAMP cascade. J. Biol. Chem. *263*, 8576–8582.

Verna, J., Lodder, A., Lee, K., Vagts, A., and Ballester, R. (1997). A family of genes required for maintenance of cell wall integrity and for the stress response in *Saccharomyces cerevisiae*. Proc. Natl. Acad. Sci. USA *94*, 13804–13809.

Wach, A., Brachat, A., Pohlmann, R., and Philippsen, P. (1994). New heterologous modules for classical or PCR-based gene disruptions in *Saccharomyces cerevisiae*. Yeast *10*, 1793–1808.

Wade, J. T., Hall, D. B., and Struhl, K. (2004). The transcription factor Ifh1 is a key regulator of yeast ribosomal protein genes. Nature *432*, 1054–1058.

Watanabe, Y., Takaesu, G., Hagiwara, M., Irie, K., and Matsumoto, K. (1997). Characterization of a serum response factor-like protein in *Saccharomyces cerevisiae*, Rlm1, which has transcriptional activity regulated by the Mpk1 (Slt2) mitogen-activated protein kinase pathway. Mol. Cell. Biol. *17*, 2615–2623.

Wei, Y., Tsang, C. K., and Zheng, X. F. (2009). Mechanisms of regulation of RNA polymerase III-dependent transcription by TORC1. EMBO J. *28*, 2220–2230.

Werner-Washburne, M., Brown, D., and Braun, E. (1991). Bcy1, the regulatory subunit of cAMP-dependent protein kinase in yeast, is differentially modified in response to the physiological status of the cell. J. Biol. Chem. *266*, 19704–19709.

Wilson-Grady, J. T., Villen, J., and Gygi, S. P. (2008). Phosphoproteome analysis of fission yeast. J. Proteome Res. *7*, 1088–1097.

Wullschleger, S., Loewith, R., and Hall, M. N. (2006). TOR signaling in growth and metabolism. Cell *124*, 471–484.

Xie, M. W., Jin, F., Hwang, H., Hwang, S., Anand, V., Duncan, M. C., and Huang, J. (2005). Insights into TOR function and rapamycin response: chemical genomic profiling by using a high-density cell array method. Proc. Natl. Acad. Sci. USA *102*, 7215–7220.

Zappacosta, F., Huddleston, M. J., Karcher, R. L., Gelfand, V. I., Carr, S. A., and Annan, R. S. (2002). Improved sensitivity for phosphopeptide mapping using capillary column HPLC and microionspray mass spectrometry: comparative phosphorylation site mapping from gel-derived proteins. Anal. Chem. *74*, 3221–3231.

Zheng, L., Baumann, U., and Reymond, J. L. (2004). An efficient one-step site-directed and site-saturation mutagenesis protocol. Nucleic Acids Res. *32*, e115.

Zurita-Martinez, S. A., and Cardenas, M. E. (2005). Tor and cyclic AMP-protein kinase A: two parallel pathways regulating expression of genes required for cell growth. Eukaryot. Cell *4*, 63–71.